Seismic interferometry by cross-correlation or deconvolution?

Kees Wapenaar*, Joost van der Neut, Elmer Ruigrok, Deyan Draganov, Evert Slob, Jan Thorbecke, Delft University of Technology, and Roel Snieder, Colorado School of Mines

SUMMARY

We discuss Rodney Calvert's work on the Virtual Source method in the context of seismic interferometry. Moreover, we present a systematic analysis of seismic interferometry by cross-correlation versus multi-dimensional deconvolution and we discuss applications of both approaches.

INTRODUCTION

Because of his lively creativity and intense personal interest in others, Rodney Calvert left a lasting professional and personal imprint in geophysics. During the 2004 SEG convention he introduced the virtual source (VS) method to the geophysical community, together with his colleague Andrey Bakulin (Bakulin and Calvert, 2004). In essence, the VS method is an elegant data-based alternative to model-based redatuming. For an acquisition configuration with sources at the surface and receivers in the subsurface, for example in a horizontal borehole, the direct arrivals observed by the downhole receivers can be seen as a measured version of a wavefield extrapolation operator. Redatuming thus boils down to cross-correlating these direct arrivals with the observed reflection events in the borehole and summing the results over the different sources at the surface, according to

$$D_{\alpha\beta}(t) = \sum_{k=1}^{N} S_{k\alpha}(-t) * S_{k\beta}(t) \qquad (1)$$

($*$ denotes temporal convolution). The result $D_{\alpha\beta}(t)$ is equivalent with the response of a virtual downhole source (α), measured by any downhole receiver (β). In this VS response, the distortions due to the inhomogeneous overburden are removed, without needing any knowledge of the overburden macro model. The idea of replacing a model-based operator by a 'measured operator' $S_{k\alpha}(-t)$ may seem simple with hindsight, but the consequences are far reaching. Bakulin et al. (2007) give an impressive overview of the applications in imaging and reservoir monitoring.

The 2004 SEG presentation was delivered at a time when other researchers in seismology (exploration and non-exploration), underwater acoustics and ultrasonics were independently pioneering 'Green's function retrieval by cross-correlation', also known as seismic interferometry, with applications for passive as well as controlled-source data. In recent years there has grown an intensive cross-fertilization between these fields, including the VS method. The SEG reprint book 'Seismic interferometry, history and present status' (2008) gives an overview of this rapidly expanding field of research.

Recently it has been recognized that in many situations it can be advantageous to replace the correlation process by deconvolution. One of the advantages is that deconvolution compensates for the properties of the source wavelet; another advantage is that it is not necessary to assume that the medium is lossless. Bakulin and Calvert (2006) propose to replace their operator $S_{k\alpha}(-t)$ by $S_{k\alpha}^{-1}(t)$ to compensate for variations in the source wavelet and reverberations in the overburden. Snieder et al. (2006a) deconvolve passive wave fields observed at different depth levels and show that this changes the boundary conditions of a system. They applied it to earthquake data recorded at different heights in the Millikan library in Pasadena and obtained the impulse response of the building. Mehta et al. (2007) used a similar approach to estimate the near-surface properties of the Earth from passive recordings in a vertical borehole. Vasconcelos and Snieder (2006, 2007) and Vasconcelos et al. (2007) used deconvolution interferometry in seismic imaging with complicated and unknown source-time signals and for imaging with internal multiples. All these approaches essentially employ a 1-D deconvolution process.

Various authors have shown that multi-dimensional deconvolution (MDD), applied to controlled-source data with receivers at a constant depth level (for example at the ocean bottom or in a horizontal borehole), can also be used to change the boundary conditions of a system. Wapenaar and Verschuur (1996) and Amundsen (1999) use MDD of wavefields recorded at the ocean bottom to obtain the response of the subsurface without ocean-bottom and surface related multiples. Berkhout's data processing in the inverse data space (Berkhout, 2006) is another form of multi-dimensional deconvolution. Schuster and Zou (2006) and Wapenaar et al. (2008a) discuss MDD of controlled-source data in the context of seismic interferometry. Slob et al. (2007) apply MDD to modelled CSEM data and demonstrate the insensitivity to dissipation as well as the potential of changing the boundary conditions: the effect of the air wave, a notorious problem in CSEM prospecting, is largely suppressed.

The aim of this paper is to give a systematic analysis of seismic interferometry by cross-correlation versus multi-dimensional deconvolution and to discuss applications of both approaches.

GENERAL EXPRESSIONS

We use a unified notation to facilitate our discussion of the different approaches. The general expression for interferometry by cross-correlation is given by

$$C(\mathbf{x}_B, \mathbf{x}_A, t) = \int p(\mathbf{x}_B, \mathbf{x}_S, t) * q(\mathbf{x}_A, \mathbf{x}_S, -t)\mathrm{d}\mathbf{x}_S. \qquad (2)$$

The form of this equation is equivalent with that of equation 1, except that the order of terms and arguments is reversed. The quantities $p(\mathbf{x}_B, \mathbf{x}_S, t)$ and $q(\mathbf{x}_A, \mathbf{x}_S, t)$ represent responses of a source at $\mathbf{x}_S$, observed at receivers $\mathbf{x}_B$ and $\mathbf{x}_A$, respectively; these responses will be specified later for different situations. For each situation the correlation function $C(\mathbf{x}_B, \mathbf{x}_A, t)$ is related in a specific way to the Green's function $G(\mathbf{x}_B, \mathbf{x}_A, t)$. Hence, equation 2 can be seen as an *explicit* Green's function representation.

The general expression for interferometry by MDD reads

$$u(\mathbf{x}_B, \mathbf{x}_S, t) = \int D(\mathbf{x}_B, \mathbf{x}_A, t) * v(\mathbf{x}_A, \mathbf{x}_S, t)\mathrm{d}\mathbf{x}_A, \qquad (3)$$

with responses $u(\mathbf{x}_B, \mathbf{x}_S, t)$ and $v(\mathbf{x}_A, \mathbf{x}_S, t)$ to be discussed later for different situations. For each situation the function $D(\mathbf{x}_B, \mathbf{x}_A, t)$ is related in a specific way to the Green's function $G(\mathbf{x}_B, \mathbf{x}_A, t)$. Hence, equation 3 can be seen as an *implicit* Green's function representation. Resolving D from equation 3 involves multi-dimensional deconvolution. Hence, $D(\mathbf{x}_B, \mathbf{x}_A, t)$ is called the deconvolution function.

It turns out to be convenient to analyze both approaches in the frequency domain. Defining the Fourier transform of a time-dependent function $p(t)$ as $\hat{p}(\omega) = \int_{-\infty}^{\infty} \exp(-j\omega t) p(t) dt$, with j the imaginary unit and ω the angular frequency, we obtain

$$\hat{C}(\mathbf{x}_B, \mathbf{x}_A, \omega) = \int \hat{p}(\mathbf{x}_B, \mathbf{x}_S, \omega) \hat{q}^*(\mathbf{x}_A, \mathbf{x}_S, \omega) d\mathbf{x}_S \quad (4)$$

(superscript $*$ denotes complex conjugation) and

$$\hat{u}(\mathbf{x}_B, \mathbf{x}_S, \omega) = \int \hat{D}(\mathbf{x}_B, \mathbf{x}_A, \omega) \hat{v}(\mathbf{x}_A, \mathbf{x}_S, \omega) d\mathbf{x}_A, \quad (5)$$

respectively. The implementation of equation 4 involves a discretization of $\hat{p}$ and $\hat{q}$ and replacing the integral along the source coordinate $\mathbf{x}_S$ by a summation (as in virtual source equation 1); for an accurate discretization the source points $\mathbf{x}_S$ should be regularly distributed. Note that in principle it is sufficient to have single receiver points $\mathbf{x}_A$ and $\mathbf{x}_B$.

The process to resolve $\hat{D}(\mathbf{x}_B, \mathbf{x}_A, \omega)$ from equation 5 is more involved. Discretization of this equation requires an array of regularly distributed receiver points $\mathbf{x}_A$ (or else a grid of receivers that is dense enough to allow regularization). Inversion of this equation requires multiple source points $\mathbf{x}_S$, not necessarily regularly distributed. Note that in principle it is sufficient to have a single receiver point $\mathbf{x}_B$. After discretization, $\hat{u}$ and $\hat{v}$ can be stored in matrices $\hat{\mathbf{U}}$ and $\hat{\mathbf{V}}$, respectively. For example, a column of $\hat{\mathbf{V}}$ contains $\hat{v}(\mathbf{x}_A, \mathbf{x}_S, \omega)$ for a fixed source position $\mathbf{x}_S$ and variable receiver position $\mathbf{x}_A$; a row of $\hat{\mathbf{V}}$ contains $\hat{v}(\mathbf{x}_A, \mathbf{x}_S, \omega)$ for a fixed receiver position $\mathbf{x}_A$ and variable source position $\mathbf{x}_S$ (Berkhout, 1982). Equation 5 thus becomes

$$\hat{\mathbf{U}} = \hat{\mathbf{D}}\hat{\mathbf{V}}, \quad (6)$$

with $\hat{\mathbf{D}}$ being the discretized version of the deconvolution function $\hat{D}(\mathbf{x}_B, \mathbf{x}_A, \omega)$. $\hat{\mathbf{D}}$ can now be resolved for example via weighted least-squares inversion, according to

$$\hat{\mathbf{D}} = \hat{\mathbf{U}}\mathbf{W}\hat{\mathbf{V}}^{\dagger}\left(\hat{\mathbf{V}}\mathbf{W}\hat{\mathbf{V}}^{\dagger} + \epsilon^2 \mathbf{I}\right)^{-1}, \quad (7)$$

where the superscript $\dagger$ denotes transposition and complex conjugation, $\mathbf{W}$ is a diagonal weighting matrix, $\mathbf{I}$ the identity matrix and ϵ^2 a stabilization parameter. Applying equation 7 for each frequency component and transforming the result back to the time domain is equivalent with MDD in the time domain.

For the sake of comparison with the correlation approach, let us see what happens when we replace the inverse matrix in equation 7 by $\hat{S}^{-1}(\omega)$, where $\hat{S}(\omega)$ is some average power spectrum. For convenience we also skip the weighting matrix. Equation 7 thus becomes

$$\hat{\mathbf{D}} \approx \hat{\mathbf{U}}\hat{\mathbf{V}}^{\dagger}/\hat{S}(\omega). \quad (8)$$

Rewritten in integral form this gives

$$\hat{D}(\mathbf{x}_B, \mathbf{x}_A, \omega)\hat{S}(\omega) \approx \int \hat{u}(\mathbf{x}_B, \mathbf{x}_S, \omega)\hat{v}^*(\mathbf{x}_A, \mathbf{x}_S, \omega) d\mathbf{x}_S.$$
$$(9)$$

Note the analogy with equation 4. In the following we encounter situations for which $\hat{p} = \hat{u}$ and $\hat{q} = \hat{v}$. For those situations the cross-correlation approach of equation 4 is an approximation of the deconvolution approach of equation 7. We will also encounter situations for which $\hat{p}$ and $\hat{q}$ are not equal to $\hat{u}$ and $\hat{v}$. In those situations the cross-correlation and deconvolution approaches are complementary.

SEISMIC INTERFEROMETRY BY CROSSCORRELATION

We briefly review the theory for seismic interferometry by cross-correlation. Assuming an arbitrary closed surface $\partial\mathbb{D}$ enclosing two observation points $\mathbf{x}_A$ and $\mathbf{x}_B$ in an arbitrary inhomogeneous lossless medium, the representation for the acoustic Green's function between those two points reads (Wapenaar et al., 2005; van Manen et al., 2005)

$$2\Re\{\hat{G}(\mathbf{x}_B, \mathbf{x}_A, \omega)\} \approx \quad (10)$$
$$\frac{2}{\rho c} \oint_{\partial\mathbb{D}} \hat{G}(\mathbf{x}_B, \mathbf{x}_S, \omega)\hat{G}^*(\mathbf{x}_A, \mathbf{x}_S, \omega) d\mathbf{x}_S,$$

where ρ and c are the mass density and propagation velocity of the medium at and outside $\partial\mathbb{D}$. Note that the integration takes place along sources at $\mathbf{x}_S$ on $\partial\mathbb{D}$. The approximation sign refers to high-frequency and far-field approximations, mainly resulting in amplitude errors. Equation 10 accounts not only for the direct wave, but also for primary and multiple scattering. Note that the inverse Fourier transform of the left-hand side gives $G(\mathbf{x}_B, \mathbf{x}_A, t) + G(\mathbf{x}_B, \mathbf{x}_A, -t)$. By extracting the causal part we obtain the Green's function $G(\mathbf{x}_B, \mathbf{x}_A, t)$.

Transient sources

When the sources are transients $s(\mathbf{x}_S, t)$, with spectra $\hat{s}(\mathbf{x}_S, \omega)$, equation 10 can be rewritten as

$$2\Re\{\hat{G}(\mathbf{x}_B, \mathbf{x}_A, \omega)\}\hat{S}(\omega) \approx \quad (11)$$
$$\frac{2}{\rho c} \oint_{\partial\mathbb{D}} \hat{\mathcal{F}}(\mathbf{x}_S, \omega)\hat{p}^{\text{obs}}(\mathbf{x}_B, \mathbf{x}_S, \omega)\hat{p}^{\text{obs}*}(\mathbf{x}_A, \mathbf{x}_S, \omega) d\mathbf{x}_S,$$

where $\hat{S}(\omega)$ is some average (arbitrarily chosen) power spectrum, $\hat{\mathcal{F}}(\mathbf{x}_S, \omega)$ is a shaping filter, defined as $\hat{\mathcal{F}}(\mathbf{x}_S, \omega) = \hat{S}(\omega)/\{\hat{s}(\mathbf{x}_S, \omega)\hat{s}^*(\mathbf{x}_S, \omega)\}$, and $\hat{p}^{\text{obs}}(\mathbf{x}_A, \mathbf{x}_S, \omega)$ denotes the observed acoustic pressure at $\mathbf{x}_A$, due to a source at $\mathbf{x}_S$, according to $\hat{p}^{\text{obs}}(\mathbf{x}_A, \mathbf{x}_S, \omega) = \hat{G}(\mathbf{x}_A, \mathbf{x}_S, \omega)\hat{s}(\mathbf{x}_S, \omega)$ (and a similar expression for $\hat{p}^{\text{obs}}(\mathbf{x}_B, \mathbf{x}_S, \omega)$).

Noise sources

When the sources are uncorrelated noise $\hat{N}(\mathbf{x}_S, \omega)$, with $\langle \hat{N}(\mathbf{x}_S, \omega)\hat{N}^*(\mathbf{x}'_S, \omega) \rangle = \delta_{2D}(\mathbf{x}_S - \mathbf{x}'_S)\hat{S}(\omega)$, equation 10 reduces to

$$2\Re\{\hat{G}(\mathbf{x}_B, \mathbf{x}_A, \omega)\}\hat{S}(\omega) \approx \frac{2}{\rho c}\langle\hat{p}^{\text{obs}}(\mathbf{x}_B, \omega)\hat{p}^{\text{obs}*}(\mathbf{x}_A, \omega)\rangle,$$
$$(12)$$

where $\hat{p}^{\text{obs}}(\mathbf{x}_A, \omega)$ denotes the observed acoustic pressure at $\mathbf{x}_A$, according to

$$\hat{p}^{\text{obs}}(\mathbf{x}_A, \omega) = \oint_{\partial\mathbb{D}} \hat{G}(\mathbf{x}_A, \mathbf{x}_S, \omega)\hat{N}(\mathbf{x}_S, \omega) d\mathbf{x}_S \quad (13)$$

(and a similar expression for $\hat{p}^{\text{obs}}(\mathbf{x}_B, \omega)$).

Passive data

For passive data we consider the configuration of Figure 1a. Here $\partial\mathbb{D}$ consists of a free surface $\partial\mathbb{D}_0$ and an arbitrarily shaped surface $\partial\mathbb{D}_m$ in the subsurface. The integration can now be restricted to sources on $\partial\mathbb{D}_m$ (transients or noise).

For the situation of noise sources, the modification of equation 12 for the elastodynamic Green's tensor reads (Wapenaar and Fokkema, 2006)

$$2\Re\{\hat{G}_{ij}(\mathbf{x}_B, \mathbf{x}_A, \omega)\}\hat{S}(\omega) \approx \frac{2}{\rho c_P}\langle\hat{v}_i^{\mathrm{obs}}(\mathbf{x}_B, \omega)\hat{v}_j^{\mathrm{obs}*}(\mathbf{x}_A, \omega)\rangle,\tag{14}$$

where $\hat{v}_i^{\mathrm{obs}}$ is the particle velocity, observed by seismometers or geophones (usually at or close to the free surface). Equation 14 explains the retrieval of surface waves traveling between $\mathbf{x}_A$ and $\mathbf{x}_B$ (Campillo and Paul, 2003; Gerstoft et al., 2006), and has also been used to retrieve the reflection response from passive data (Draganov et al., 2007).

Controlled-source data

For controlled-source data we consider the configuration of Figure 1b. The sources are at $\partial\mathbb{D}_0$, which is now assumed to be a reflection free surface (this assumption is satisfied after application of surface-related multiple elimination). The integral in equation 11 can now only be taken over $\partial\mathbb{D}_0$. This leads to spurious events (Snieder et al., 2006b), unless the medium is 'sufficiently inhomogeneous' so that the integral over $\partial\mathbb{D}_m$ vanishes (Wapenaar, 2006). In the virtual source method the spurious events are partly suppressed by replacing $\hat{p}^{\mathrm{obs}}(\mathbf{x}_A, \mathbf{x}_S, \omega)$ in equation 11 by the direct arrival, which is obtained by applying a window in the time-domain (Bakulin and Calvert, 2006). Mehta et al. (2007a) improved this further by applying up/down wavefield separation. Equation 11 thus becomes (omitting for convenience the shaping filter and the factor $2/\rho c$)

$$\hat{R}_0^+(\mathbf{x}_B, \mathbf{x}_A, \omega)\hat{S}(\omega) \approx \tag{15}$$
$$\int_{\partial\mathbb{D}_0}\hat{p}^-(\mathbf{x}_B, \mathbf{x}_S, \omega)\{\hat{p}_{\mathrm{dir}}^+(\mathbf{x}_A, \mathbf{x}_S, \omega)\}^*\mathrm{d}\mathbf{x}_S,$$

where the superscripts $+$ and $-$ stand for down going and up going, respectively. Note that in the left-hand side we replaced the Green's function by the reflection response for down going waves and we removed the $\Re$-sign (the decomposition breaks the time symmetry). We will see later that a further improvement is possible by applying multi-dimensional deconvolution (MDD).

SEISMIC INTERFEROMETRY BY DECONVOLUTION

The expressions for seismic interferometry by cross-correlation in the previous section were in essence all derived from the same Green's function representation (equation 10, or its elastodynamic equivalent). The resulting expressions had the form of equation 4. The following discussion on seismic interferometry by MDD is less systematic. On a case-by-case basis we will discuss implicit representations of the form of equation 5.

Controlled-source data with horizontal arrays

For OBC data it turns out that the relation between down going and up going waves $\hat{p}^+$ and $\hat{p}^-$ just below the ocean
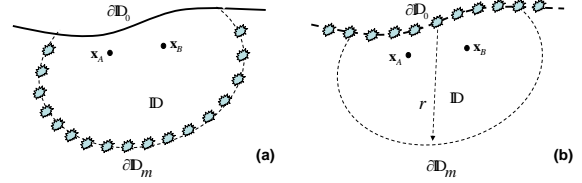

Fig. 1: *Configuration for (a) passive and (b) controlled-source interferometry.*

bottom ($\partial\mathbb{D}_1$) can be written as

$$\hat{p}^-(\mathbf{x}_B, \mathbf{x}_S, \omega) = \int_{\partial\mathbb{D}_1}\hat{R}_0^+(\mathbf{x}_B, \mathbf{x}_A, \omega)\hat{p}^+(\mathbf{x}_A, \mathbf{x}_S, \omega)\mathrm{d}\mathbf{x}_A\tag{16}$$

(Wapenaar and Verschuur, 1996; Amundsen, 1999; Wapenaar et al., 2000; Osen and Amundsen, 2001; Schuster and Zhou, 2006). Here $\hat{R}_0^+(\mathbf{x}_B, \mathbf{x}_A, \omega)$ is the reflection response of the 3-D inhomogeneous dissipative medium below the ocean bottom, without any multiples related to the ocean bottom and the water surface. Assuming there are multiple source points $\mathbf{x}_S$ above the ocean bottom, $\hat{R}_0^+(\mathbf{x}_B, \mathbf{x}_A, \omega)$ is resolved from equation 16 following the procedure discussed below equation 5. Although originally derived for seismic data, the same procedure can be applied to CSEM data (Slob et al., 2007). In that case $\hat{p}^+$ and $\hat{p}^-$ denote electric diffusion fields, decaying in the positive and negative depth direction, respectively.

The horizontal array is not necessarily located at the ocean bottom, but it can also be a horizontal borehole. In that case equation 16 can be seen as a further improvement of the virtual source method described by equation 15, see also the remarks below equation 9. Van der Neut et al. (2008) show that the elastodynamic extension of this approach has the potential to correct for source directivity of pressure and shear sources.

Passive transient data with horizontal arrays

For the situation of passive data of buried transient sources, observed at the free surface $\partial\mathbb{D}_0$, we obtain (Wapenaar et al., 2008b)

$$\Delta\hat{v}_3(\mathbf{x}_B, \mathbf{x}_S, \omega) = \int_{\partial\mathbb{D}_0}\hat{G}_{33}(\mathbf{x}_B, \mathbf{x}_A, \omega)\hat{\bar{p}}(\mathbf{x}_A, \mathbf{x}_S, \omega)\mathrm{d}\mathbf{x}_A,\tag{17}$$

with $\Delta\hat{v}_3(\mathbf{x}_B, \mathbf{x}_S, \omega) = \hat{\bar{v}}_3(\mathbf{x}_B, \mathbf{x}_S, \omega) - \hat{v}_3(\mathbf{x}_B, \mathbf{x}_S, \omega)$ (particle velocity) and $\hat{\bar{p}}$ standing for acoustic pressure. The bars denote reference fields in the actual medium, but without the free surface. In specific situations these responses can be obtained from $\hat{v}_3(\mathbf{x}_B, \mathbf{x}_S, \omega)$ by applying a window in the time domain. Comparing the fields in equation 17 with those in equation 11 we observe that these fields are different, hence equations 11 and 17 are complementary, see also the remarks below equation 9. For the configuration shown in Figure 2 we applied interferometry by cross-correlation (equation 11 without the shaping filter) and by MDD (i.e., resolving $\hat{G}_{33}(\mathbf{x}_B, \mathbf{x}_A, \omega)$ from equation 17 using equation 7). The results, shown in Figure 3, confirm that MDD has the potential to correct for irregular source distributions. Possible applications are reservoir characterization with microseismic data and improvement of crustal imaging with teleseismic data (Shragge et al., 2006; Kumar and Bostock, 2006).

Passive noise data with horizontal arrays
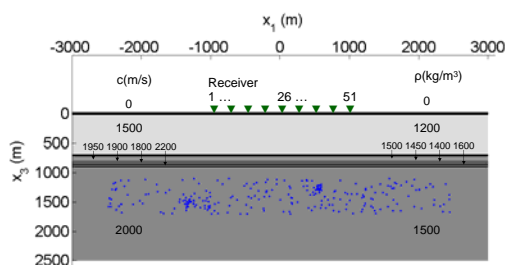
Returning to equation 16 one may wonder whether

Fig. 2: *Layered target below a homogeneous overburden and a free surface. The irregularly distributed sources below the target sequentially emit transient signals with different spectra.*

$\hat{R}_0^+(\mathbf{x}_B, \mathbf{x}_A, \omega)$ can be resolved when $\hat{p}^+$ and $\hat{p}^-$ are continuous noise signals from a distribution of sources above $\partial \mathbb{D}_1$. In that case $\hat{U}$ and $\hat{V}$ in equation 6 are vectors instead of matrices, but this does not prevent $\hat{D}$ to be resolved using equation 7. Since the noise signals should be very long (similar as in the cross-correlation method), the computational cost will be significant. Potential applications are e.g. the retrieval of virtual CSEM data from magnetotelluric noise (low-frequency) as well as virtual GPR data from extraterrestrial electromagnetic noise (high-frequency).

Controlled-source data with vertical arrays

Willis et al. (2006), Xiao et al. (2006) and Hornby and Yu (2007) have proposed salt-flank imaging using cross-correlation interferometry applied to VSP data. For this situation interferometry by MDD is also an option. Equation 16 holds for this situation, with $\partial \mathbb{D}_1$ representing the borehole, $\hat{p}^+$ the wavefield propagating towards the salt-flank and $\hat{p}^-$ the reflected field (see Figure 4a). Hence, the reflection response of the salt-flank can be resolved by MDD, using equation 7.

Minato et al. (2007) discuss cross-well seismic imaging with cross-correlation interferometry. To apply interferometry by MDD for this situation we modify equation 16 as follows

$$\hat{p}^+(\mathbf{x}_B, \mathbf{x}_S, \omega) = \int_{\partial \mathbb{D}_1} \hat{G}^+(\mathbf{x}_B, \mathbf{x}_A, \omega) \hat{p}^+(\mathbf{x}_A, \mathbf{x}_S, \omega) d\mathbf{x}_A,$$

(18)

where $\hat{p}^+(\mathbf{x}_A, \mathbf{x}_S, \omega)$ and $\hat{p}^+(\mathbf{x}_B, \mathbf{x}_S, \omega)$ represent 'rightward propagating' one-way wavefields in the two wells (see Figure 4b), and $\hat{G}^+(\mathbf{x}_B, \mathbf{x}_A, \omega)$ is the one-way Green's function, which can be resolved by MDD.

Passive data with vertical arrays

Cross-correlation methods have also been proposed for vertical arrays in oceanic waveguides (Roux and Fink, 2003; Sabra et al., 2005b; Brooks and Gerstoft, 2007). This situation is comparable with the cross-well method in seismics, but with the transient sources replaced by noise sources. For this situation MDD involves resolving $\hat{G}^+(\mathbf{x}_B, \mathbf{x}_A, \omega)$ from equation 18 using equation 7, with $\hat{U}$ and $\hat{V}$ being vectors instead of matrices.

Surface waves with regular arrays

Consider a regularly sampled array of seismometers, like in the USArray, illuminated mainly from one direction (Sabra et al., 2005a; Shapiro et al., 2005). Assuming surface waves can be approximately described by a 2D wave equation with a 2D inhomogeneous dispersive Rayleigh wave velocity, interferometry by MDD can be applied by resolving the Rayleigh wave Green's function $\hat{G}^+(\mathbf{x}_B, \mathbf{x}_A, \omega)$ from equation 18.
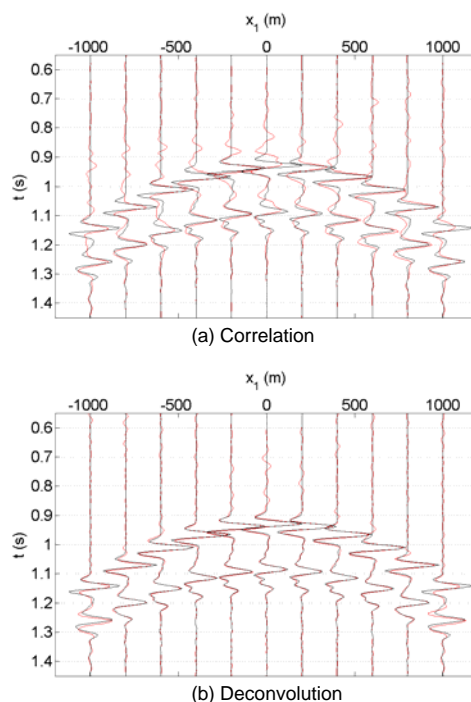

(a) Correlation

(b) Deconvolution

Fig. 3: *(a) Result of interferometry by cross-correlation (red traces) compared with the directly modeled response of a source at $\mathbf{x} = \mathbf{0}$ (black traces). (b) Result of interferometry by multi-dimensional deconvolution (MDD).*
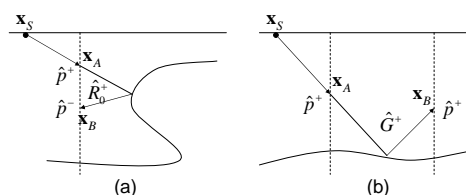

Fig. 4: *Configuration for MDD with vertical arrays.*

CONCLUSIONS

We discussed seismic interferometry by cross-correlation as well as by multi-dimensional deconvolution (MDD). The main advantage of MDD is its relative insensitivity for irregular source distributions. Moreover, it can be applied in dissipative media. Unlike in the cross-correlation method, in MDD the responses at all receivers are simultaneously involved in the matrix inversion. This matrix inversion makes MDD more costly than cross-correlation. Moreover, it requires a regular receiver grid, or at least a grid that is dense enough to allow regularization.

The choice for applying seismic interferometry by cross-correlation or by MDD depends on many factors. Despite the mentioned limitations of MDD, we believe that its relative insensitivity for irregularities in the source distribution as well as its applicability for dissipative media makes it an attractive approach for various applications, ranging from reservoir imaging and characterization using microseismic data to GPR imaging using extraterrestrial electromagnetic noise.

EDITED REFERENCES
Note: This reference list is a copy-edited version of the reference list submitted by the author. Reference lists for the 2008 SEG Technical Program Expanded Abstracts have been copy edited so that references provided with the online metadata for each paper will achieve a high degree of linking to cited sources that appear on the Web.

REFERENCES

Amundsen, L., 1999, Elimination of free surface-related multiples without need of the source wavelet: 69th Annual International Meeting, SEG, Expanded Abstracts, 1064–1067.

Bakulin, A., and R. Calvert, 2004, Virtual source: New method for imaging and 4D below complex overburden: 74th Annual International Meeting, SEG, Expanded Abstracts, 2477–2480.

———2006, The virtual source method: Theory and case study: Geophysics, **71**, SI139–SI150.

Bakulin, A., A. Mateeva, K. Mehta, P. Jorgensen, J. Ferrandis, I. Sinha-Herhold, and J. Lopez, 2007, Virtual source applications to imaging and reservoir monitoring: The Leading Edge, **26**, 732–740.

Berkhout, A. J., 1982, Seismic migration: Imaging of acoustic energy by wavefield extrapolation: Elsevier.

———2006, Seismic processing in the inverse data space: Geophysics, **71**, A29–A33.

Brooks, L. A., and P. Gerstoft, 2007, Ocean acoustic interferometry: Journal of the Acoustical Society of America, **121**, 3377–3385.

Campillo, M., and A. Paul, 2003, Long-range correlations in the diffuse seismic coda: Science, **299**, 547–549.

Draganov, D., K. Wapenaar, W. Mulder, J. Singer, and A. Verdel, 2007, Retrieval of reflections from seismic background-noise measurements: Geophysysical Research Letters, **34**, L04305.

Gerstoft, P., K. G. Sabra, P. Roux, W. A. Kuperman, and M. C. Fehler, 2006, Green's functions extraction and surface-wave tomography from microseisms in southern California: Geophysics, **71**, SI23–SI31.

Hornby, B. E., and J. Yu, 2007, Interferometric imaging of a salt flank using walkaway VSP data: The Leading Edge, **26**, 760–763.

Kumar, M. R. and M. G. Bostock, 2006, Transmission to reflection transformation of teleseismic wavefields: Journal of Geophysical Research—Solid Earth, **111**, B08306.

Mehta, K., A. Bakulin, J. Sheiman, R. Calvert, and R. Snieder, 2007a, Improving the virtual source method by wavefield separation: Geophysics, **72**, V79–V86.

Mehta, K., R. Snieder, and V. Graizer, 2007b, Extraction of near-surface properties for a lossy layered medium using the propagator matrix: Geophysical Journal International, **169**, 271–280.

Minato, S., K. Onishi, T. Matsuoka, Y. Okajima, J. Tsuchiyama, D. Nobuoka, H. Azuma, and T. Iwamoto, 2007, Cross-well seismic survey without borehole source: 77th Annual International Meeting, SEG, Expanded Abstracts, 1357–1361.

Osen, A., and L. Amundsen, 2001, Multidimensional multiple attenuation of OBS data: 71st Annual International Meeting, SEG, Expanded Abstracts, 817–820.

Roux, P., and M. Fink, 2003, Green's function estimation using secondary sources in a shallow water environment: Journal of the Acoustical Society of America, **113**, 1406–1416.

Sabra, K. G., P. Gerstoft, P. Roux, W. A. Kuperman, and M. C. Fehler, 2005a, Surface wave tomography from microseisms in Southern California: Geophysysical Research Letters, **32**, L14311.

Sabra, K. G., P. Roux, and W. A. Kuperman, 2005b, Arrival-time structure of the time-averaged ambient noise cross-correlation function in an oceanic waveguide: Journal of the Acoustical Society of America, **117**, 164–174.

Schuster, G. T., and M. Zhou, 2006, A theoretical overview of model-based and correlation-based redatuming methods: Geophysics, **71**, SI103–SI110.

Shapiro, N. M., M. Campillo, L. Stehly, and M. H. Ritzwoller, 2005, High-resolution surface-wave tomography from ambient seismic noise: Science, **307**, 1615–1618.

Shragge, J., B. Artman, and C. Wilson, 2006, Teleseismic shot-profile migration: Geophysics, **71**, SI221–SI229.

Slob, E., K. Wapenaar, and R. Snieder, 2007, Interferometry in dissipative media: Addressing the shallow sea problem for seabed logging applications: 77th Annual International Meeting, SEG, Expanded Abstracts, 559–563.

Snieder, R., J. Sheiman, and R. Calvert, 2006a, Equivalence of the virtual-source method and wave-field deconvolution in seismic interferometry: Physical Review E, **73**, 066620.

Snieder, R., K. Wapenaar, and K. Larner, 2006b, Spurious multiples in seismic interferometry of primaries: Geophysics, **71**, SI111–SI124.

Van der Neut, J., K. Wapenaar, and E. Slob, 2008, Multicomponent controlled-source interferometry by multidimensional deconvolution applied to a 1D elastic model: Presented at the 70th Annual International Conference and Exhibition, EAGE.

van Manen, D.-J., J.O.A. Robertsson, and A. Curtis, 2005, Modeling of wave propagation in inhomogeneous media: Physical Review Letters, **94**, 164301.

Vasconcelos, I., and R. Snieder, 2006, Interferometric imaging by deconvolution: Theory and numerical examples: 76th Annual International Meeting, SEG, Expanded Abstracts, 2416–2420.

———2007, Seismic interferometry by deconvolution: theory and examples: 69th Annual Interncational Conference and Exhibition, EAGE, Extended Abstracts, H001.

Vasconcelos, I., R. Snieder, and B. Hornby, 2007, Target-oriented interferometry: Imaging with internal multiples from subsalt VSP data: 77th Annual International Meeting, SEG, Expanded Abstracts, 3069–3073.

Wapenaar, K., 2006, Green's function retrieval by cross-correlation in case of one-sided illumination: Geophysysical Research Letters, **33**, L19304.

Wapenaar, K., and J. Fokkema, 2006, Green's function representations for seismic interferometry: Geophysics, **71**, SI33–SI46.

Wapenaar, K., J. Fokkema, M. Dillen, and P. Scherpenhuijsen, 2000, One-way acoustic reciprocity and its applications in multiple elimination and time-lapse seismics: 70th Annual International Meeting, SEG, Extended Abstracts, 2377–2380.

Wapenaar, K., J. Fokkema, and R. Snieder, 2005, Retrieving the Green's function in an open system by cross-correlation: a comparison of approaches (L): Journal of the Acoustical Society of America, **118**, 2783–2786.

Wapenaar, K., E. Slob, and R. Snieder, 2008a, Seismic and electromagnetic controlled-source interferometry in dissipative media: Geophysical Prospecting, **56**, in press.

Wapenaar, K., J. van der Neut, and E. Ruigrok, 2008b, Passive seismic interferometry by multidimensional deconvolution: Geophysics, **73**, submitted.

Wapenaar, C. P. A., and D. J. Verschuur, 1996, Processing of ocean bottom data: The Dolphin Project, **1**, 6.1–6.26, Delft University of Technology.

Willis, M. E., R. Lu, X. Campman, M. N. Toksöz, Y. Zhang, and M. V. de Hoop, 2006, A novel application of time-reversed acoustics: Salt-dome flank imaging using walkaway VSP surveys: Geophysics, **71**, A7–A11.

Xiao, X., M. Zhou, and G. T. Schuster, 2006, Salt-flank delineation by interferometric imaging of transmitted P- and S-waves: Geophysics, **71**, SI197–SI207.